

Level structure of ^{67}Ge and its implications for the general structure of nuclei in the $1f$ - $2p$ shell

Martin J. Murphy* and Cary N. Davids

Physics Division, Argonne National Laboratory, Argonne, Illinois 60439

(Received 21 May 1982)

From the results of prompt and β -delayed γ -ray singles and γ - γ coincidence measurements, twenty-four excited states and forty-six gamma transitions are identified in the level scheme of ^{67}Ge . Angular distributions and directional correlations of prompt ^{67}Ge gamma rays have been measured to obtain the spins of the ^{67}Ge ground state and excited states at 18.2, 122.7, 243.6, 711.3, and 1019.9 keV. Parities are assigned to the first five states on the basis of fp shell systematics and observed ^{67}Ge gamma-ray branching ratios. The 752-keV excitation energy of the first $\frac{9}{2}^+$ level in ^{67}Ge is determined from an excitation function for the $^{64}\text{Zn}(\alpha, n\gamma)^{67}\text{Ge}$ reaction. The angular distribution and correlation measurements also provide $E2/M1$ mixing ratios for the 104.4, 120.8, 122.7, 243.6, 589.0, and 897.5 keV ^{67}Ge gamma rays. The level scheme of ^{67}Ge and the corresponding schemes for $^{63,65}\text{Ni}$, $^{65,67}\text{Zn}$, and ^{69}Ge are observed to have strong similarities at low excitation. Systematic trends in $E2$ transition rates are interpreted in the context of shell and collective features of the nuclei. It is found that models based on a single particle coupled to a vibrational or deformed core do not explain the observed systematics, and are an inaccurate representation of these nuclei. The systematics do agree with a many-nucleon shell model emphasizing the short-range pairing interaction and configuration mixing for the valence neutrons.

NUCLEAR REACTIONS $^{64}\text{Zn}(\alpha, n\gamma)$, $^{63}\text{Cu}(^6\text{Li}, 2n\gamma)$, $^{58}\text{Ni}(^{14}\text{N}, \alpha n)$; ^{67}Ge level scheme, $E\gamma$, $\gamma(\theta)$, $\gamma\gamma(\theta)$, $\delta(E2/M1)$, J^π . Directional correlations with an oriented source. Ge(Li) detectors, enriched targets. Nuclear systematics, nuclear deformation.

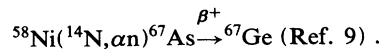
I. INTRODUCTION

This paper reports the results of an investigation of the level scheme and gamma decay of ^{67}Ge , and an analysis of structural and electromagnetic properties which ^{67}Ge shares with a group of similar odd- A nuclei in the $1f$ - $2p$ shell. The motivation for such a study was twofold: First, a planned investigation of the β^+ decay of ^{67}As required the level scheme of its β^+ decay daughter ^{67}Ge . Second, a comparison of an early, incomplete picture of the ^{67}Ge level scheme with those of $^{63,65}\text{Ni}$, $^{65,67}\text{Zn}$, and ^{69}Ge at low excitation¹ revealed similarities and systematic trends which indicate a basic structure common to all six nuclei. These nuclei have configurations which can exhibit single and many-particle shell effects, vibrational characteristics, and some aspects of collective deformation. Taken individually, the nuclei have been variously analyzed in terms of the shell model² and as single neutrons coupled to vibrational cores.^{3,4} It was anticipated that a study of the common characteristics and systematics of all six nuclei at low excitation might determine if the nuclei do behave as a single neutron coupled to a vibrational core, or if their properties are more nearly shell effects, and to what extent deformation contributes to their observed behavior. A detailed level scheme for ^{67}Ge was necessary to complete the set of data from which the systematics were extracted.

Prior to the present work, the published data on ^{67}Ge were rather sparse. Our preliminary study of low-lying levels using the $^{64}\text{Zn}(\alpha, n\gamma)^{67}\text{Ge}$ reaction¹ had yielded a ^{67}Ge mass excess of $-62\,666 \pm 12$ keV, identified twenty-

two gamma rays and four excited states (at 18.2, 122.7, 243.6, and 808.1 keV), and determined that the 18.2-keV level decayed by an $E2$ transition to the ground state. A subsequent paper by Al-Naser *et al.*⁵ confirmed the mass and the 18, 123, and 244-keV levels, and proposed sixteen additional levels. The ^{67}Ge beta-decay work by Zoller, Gordon, and Walters⁶ strongly suggested a ground state spin-parity of $\frac{1}{2}^-$; systematics of similar odd- A nuclei tentatively imply a spin sequence of $\frac{1}{2}^- - \frac{5}{2}^- - \frac{3}{2}^- - \frac{3}{2}^-$ for the ground and first three excited states. Several high spin levels above 1 MeV have been identified by Zobel *et al.*⁷ However, until now the only level below 1 MeV in ^{67}Ge whose spin had been directly measured is one depopulated by a 734-keV gamma ray: Bertschat *et al.*⁸ determined in a magnetic dipole moment measurement that the transition is from a $\frac{9}{2}^+$ state with a 70 ns half-life, but were unable to establish its excitation energy.

The ^{67}Ge level scheme reported here was established in a series of gamma-ray spectroscopy measurements. First, ^{67}Ge gamma-rays from states populated by the β^+ decay of ^{67}As were observed in singles and gamma-gamma coincidence spectra, using the reaction



Next, an excitation function of the reaction $^{64}\text{Zn}(\alpha, n\gamma)^{67}\text{Ge}$ was taken in order to obtain thresholds for fourteen of the strongest gamma transitions. In this way a framework of ^{67}Ge energy levels and associated gamma rays was obtained. The spins of the ground and first three excited states were determined from the angular distribu-

tions of five gamma rays via the reaction $^{63}\text{Cu}(^6\text{Li}, 2n\gamma)^{67}\text{Ge}$. Finally, and again using $^{63}\text{Cu} + ^6\text{Li}$, directional correlations were measured for several gamma-ray cascades. The results provided mixing ratios for five gamma rays and spin assignments to two levels above 700 keV excitation.

The measured spins of the four lowest energy states of ^{67}Ge have been found to be consistent with the patterns observed for the lowest energy states of $^{63,65}\text{Ni}$, $^{65,67}\text{Zn}$, and ^{69}Ge . The ^{67}Ge data also support further systematics in excited-state lifetimes. The nature and implications of these systematics will be discussed within the context of models of nuclear structure.

II. EXPERIMENTAL PROCEDURES

The experiments described here were carried out using ^{14}N and ^6Li ions from the Argonne FN Tandem Accelerator, and ^4He ions from the Notre Dame FN Tandem.

In order to facilitate placing ^{67}Ge gamma rays in a level scheme, an excitation function for the reaction $^{64}\text{Zn}(\alpha, n\gamma)^{67}\text{Ge}$ was measured over the range 0–2 MeV excitation in ^{67}Ge . A 1 mg/cm² enriched ^{64}Zn foil target was used, and prompt gamma rays were observed in beam with a 10% efficient Ge(Li) detector. The reaction has a laboratory threshold of 9.55 MeV (Ref. 1); to obtain the excitation function from 0 to 2 MeV the alpha projectile energy was varied from 9.500 to 11.500 MeV in 50-keV

intervals. Beam energy was calibrated using the known threshold [$E_\alpha(\text{lab})=8.640$ MeV] of the 193-keV gamma ray from $^{60}\text{Ni}(\alpha, n\gamma)^{63}\text{Zn}$, which was measured with a 3 mg/cm² ^{60}Ni foil target in a five-step excitation function from $E_\alpha=8.650$ to 8.750 MeV.

Next, the reactions $^{63,65}\text{Cu}(^6\text{Li}, 2n\gamma)^{67,69}\text{Ge}$ were used to measure the angular distributions of the 104.4, 120.8, 122.7, 243.6, and 734.0 keV ^{67}Ge gamma rays. The ^{69}Ge angular distributions were used to deduce the nuclear alignment parameter B_λ in the ^{67}Ge distributions, in order to reduce the number of free parameters (cf., Ref. 3). ^{69}Ge was produced via $^{65}\text{Cu}(^6\text{Li}, 2n\gamma)^{69}\text{Ge}$ using 15 MeV ^6Li ions and a 0.5 mg/cm² enriched ^{65}Cu foil target. The target chamber was a 4.16 cm diam aluminum cylinder with walls 0.32 cm thick and lined around the inner perimeter with a 50 mg/cm² gold foil acting as a beam stop. The target was insulated from the chamber, and the chamber was insulated from the beam line. Beam current was integrated on both the target and the chamber, which completely stopped the 15-MeV ^6Li ions. The integrated beam intensity was also monitored using the yield of the prompt 1036-keV gamma ray from ^{66}Zn , observed in a 10% Ge(Li) detector fixed at $\theta=-90^\circ$ with respect to the beam. Yields of the 232, 287, 862, and 933 keV gamma rays from ^{69}Ge were measured at 0° , 45° , and 90° with respect to the beam, using a 22 cm³ semiplanar Ge(Li)

TABLE I. Gamma rays and excited states of ^{67}Ge . E_i and E_f are the excitation energies of the initial and final states connected by E_γ .

E_γ (keV)	E_i (keV)	E_f (keV)	E_γ (keV)	E_i (keV)	E_f (keV)
18.2±0.05	18.2	0	1049.6±1.0	1293.7	243.6
104.4±0.3	122.7	18.2	1131.9±0.3	1149.6	18.2
120.8±0.3	243.6	122.7	1151.4±0.5	1274.2	122.7
122.7±0.3	122.7	0	1171.3±0.5	1293.7	122.7
217.9±0.3	929.2	711.3	1230.7±1.0	2524.0	1293.7
225.4±0.3	243.6	18.2			
243.6±0.3	243.6	0			
248.0±0.3	1900.7	1652.9	1256.7±0.3	1256.7	0
327.5±0.7	1256.7	929.2			
			1274.0±1.0	1274.2	0
437.8±0.7	1149.6	711.3			
465.0±0.7	1274.2	808.1	1294.0±0.5	1293.7	0
471.2±0.3	714.8	243.6	1309.2±1.0	1430.6	122.7
500.3±0.3	2597.0	2096.4	1385.2±1.0	2096.4	711.3
589.0±0.3	711.3	122.7	1443.4±1.0	2251.5	808.1
592.0±0.3	714.8	122.7			
			1576.7±1.0	1698.1	122.7
633.0±0.3	1652.9	1019.9	1657.0±0.5	1900.7	243.6
685.5±0.3	808.1	122.7	1698.0±0.5	1698.1	0
693.1±0.5	711.3	18.2			
			1912.8±1.0	2156.4	243.6
734.0±0.3	752.2	18.2			
776.0±0.3	1019.9	243.6			
789.9±0.3	808.1	18.2	2128.4±1.0	2251.5	122.7
807.0±1.0	929.2	122.7	2156.4±1.0	2156.4	0
808.1±0.3	808.1	0	2218.2±1.0	2218.2	0
			2280.6±1.0	2524.0	243.6
			2474.6±1.0	2597.0	122.7
897.5±0.3	1019.9	122.7			
911.0±0.5	929.2	18.2			
1036.4±0.3	1159.4	122.7			

detector 8 cm from the target. Simultaneously, the geometrical misalignment of the movable detector was measured using the yield of the prompt, isotropic 87-keV transition in ^{69}Ge .

The ^{67}Ge angular distributions were measured in the reaction $^{63}\text{Cu}(^6\text{Li}, 2n\gamma)^{67}\text{Ge}$, again using 15-MeV ^6Li ions. The target was a 1.0 mg/cm² enriched ^{63}Cu foil, and the experimental setup and geometry were identical to that in the preceding ^{69}Ge run. Integrated beam current was monitored via the prompt 991-keV gamma ray from ^{64}Zn . The yields of the prompt 104, 120, 122, 243, and 743 keV ^{67}Ge gamma rays were measured at $\theta=0^\circ$, 30° , 45° , 60° , and 90° with respect to the beam.

For the directional correlation measurement ^{67}Ge was again produced via $^{63}\text{Cu}(^6\text{Li}, 2n\gamma)^{67}\text{Ge}$, using 15-MeV ^6Li ions and the same target and chamber as in the angular distribution experiment. The directional correlations of prompt ^{67}Ge gamma-ray cascades were observed using two 10% coaxial Ge(Li) detectors operated in coincidence. Both detectors were in the same plane with the beam and 4 cm from the center of the target. One Ge(Li) was fixed at $\theta=-90^\circ$ with respect to the beam axis, and the other was moved through the three angles $\theta=0^\circ$, 45° , and 90° . The geometry corrections for source and detector mis-centering were obtained from the isotropic yields of several β -delayed gamma rays observed in singles both with the beam on and with the beam off. A further check of the entire measurement was made by observing the correlation of the well-known 807-991-keV gamma cascade from $^{63}\text{Cu}(^6\text{Li}, \alpha\gamma)^{64}\text{Zn}$.

III. RESULTS

The majority of γ rays identified in the ^{67}Ge level scheme were first observed either in the preliminary ^{67}Ge study¹ or following the decay of ^{67}As .⁹ Table I lists all of these γ rays. It also includes γ rays observed in β^+ -delayed coincidence, but which did not have sufficient intensity to be included in the ^{67}As decay scheme.

TABLE II. Excitation thresholds of ^{67}Ge γ rays from $^{64}\text{Zn}(\alpha, n\gamma)^{67}\text{Ge}$, and the assigned initial excited states of ^{67}Ge .

E_γ (keV)	Measured threshold E_α^{lab} (keV)	Measured excitation $E_{^{67}\text{Ge}}^*$ (keV)	Assigned level $E_{^{67}\text{Ge}}^*$ (keV)
217.9	10 570±40	960±45	929.2
471.2	10 280±30	690±30	714.8
589.0	10 370±35	775±35	711.3
592.0	10 340±35	750±35	714.8
685.5	10 470±40	870±40	808.1
693.1	10 295±30	705±30	711.3
734.0	10 345±35	750±35	752.2
776.0	< 10 700±45	< 1085±45	1019.9
789.9	10 370±35	770±35	808.1
897.5	< 10 685±45	< 1070±45	1019.9
1036.4	10 780±50	1160±50	1159.4
1131.9	< 10 800±50	< 1180±50	1149.6
1171.3	10 935±60	1305±60	1293.7
1256.7	10 980±60	1350±60	1256.7

A. ^{67}Ge gamma ray thresholds

The in-beam excitation function for $^{64}\text{Zn}(\alpha, n\gamma)^{67}\text{Ge}$ was used to measure the energy thresholds of gamma rays originating at levels above 250 keV in ^{67}Ge . The production cross section for gamma rays in this reaction is related to the center-of-mass projectile energy $E_\alpha^{\text{c.m.}}$ according to

$$Y_\gamma \propto \{ [E_\alpha^{\text{c.m.}} - E_0^{\text{c.m.}}(^{67}\text{Ge}) - E^*]^l + 1/2 \}, \quad (1)$$

where $-E_0^{\text{c.m.}}$ is the Q value for producing ^{67}Ge in the ground state, E^* is the energy of the initial state in the transition, and l is the orbital angular momentum carried off by the neutron.

In the energy range $0 \leq E^* \leq 2$ MeV ($9.55 \leq E_\alpha^{\text{lab}} \leq 11.55$ MeV) it was possible to obtain excitation curves for the

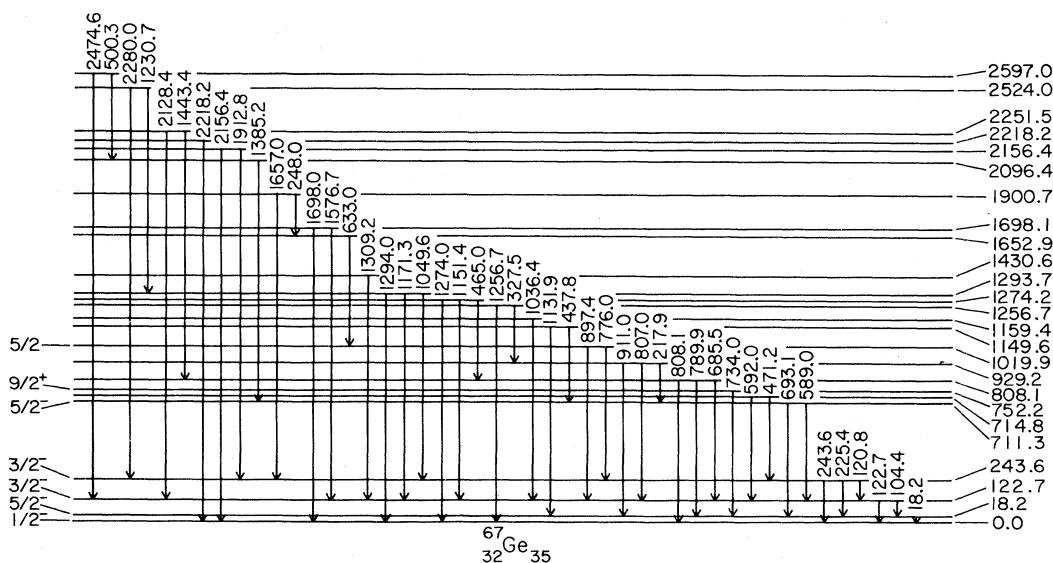


FIG. 1. The level scheme of ^{67}Ge . The spins and parities are those determined in the in-beam gamma-ray measurements.

gamma rays $E_\gamma = 217, 471, 589, 592, 685, 693, 734, 776, 789, 897, 1036, 1131, 1171, \text{ and } 1256$ keV. The net yield of each γ ray was obtained at each beam energy and corrected for dead time. Assuming that $l=0$ near threshold, these yields were fitted by linear least squares to the integrated thick target production cross section $Y_\gamma^{2/3}$ vs $E_\alpha(\text{lab})$. The resulting gamma ray thresholds are summarized in Table II. The quoted uncertainties in E_{thres} reflect a 5-keV uncertainty in beam energy, an ~ 10 -keV error from the least squares fit, and a systematic uncertainty of 20–40 keV (increasing in time during bombardment) due to carbon buildup on the target.

B. Excited states of ^{67}Ge

By combining the results of the β^+ decay and in-beam measurements, 24 ^{67}Ge excited states have been identified and 46 gamma rays placed in the level scheme shown in Fig. 1. (Table I summarizes the energy levels and gamma rays.) A study of ^{67}Ge excited states by Al-Naser *et al.*⁵ also identified the levels at 18, 122, 243, 711, 752, 929, 1020, and 1159 keV. Their data did not reveal the (weak) 685.5-keV transition, and they ascribe the 789.9-keV gamma ray to ^{67}Ga , leading them to question the existence of a level at 808.1 keV. They did observe an 807.8-keV gamma ray, and placed it as a transition between a 930-keV level and the 122.7-keV level. The excitation function reported here clearly identifies 685.5 and 789.9 keV transitions in ^{67}Ge , and in conjunction with ^{67}As beta-decay data showing a 685-keV gamma ray in coincidence with the 104 and 122 gamma rays, supports a level at 808.1 keV. The ^{67}As decay data also revealed a weak 808-keV transition in coincidence with the 122.7, but did not show the corresponding 217-keV gamma ray connected with the level at 929.2 keV. We suggest that the 808 peak is a doublet comprising an 807-keV gamma ray from the level at 929.2 (weakly fed by β^+ decay), and an 808-keV transition from the more strongly β -fed 808-keV level. A satisfactory analysis of these two transitions in prompt singles gamma-ray spectra is hampered by the strong 807-keV transition in ^{64}Zn . We also suggest that the 911-keV gamma ray observed by Al-Naser *et al.*⁵ and placed as a ground state transition is in fact a transition from the 929.2-keV level to the 18.2 isomer. The fact that Al-Naser *et al.* did not observe the 1131 gamma ray in coincidence with the 122.7 one argues against their placement of it as a $1256 \rightarrow 122.7$ transition; identifying it as $1149 \rightarrow 18.2$ resolves this conflict and is consistent with its measured threshold.

C. Results for the angular distributions

The angular distribution $W(\theta)$ of a γ ray from a nuclear level aligned in a reaction is

$$W(\theta) = 1 + A_2 B_2 Q_2 P_2(\cos\theta) + A_4 B_4 Q_4 P_4(\cos\theta). \quad (2)$$

B_λ describes the nuclear orientation, and Q_λ is the correction for detector solid angle. The A_λ are the usual angular distribution coefficients and depend on the spins of the initial and final states and the multipole mixing ratio δ of the transition.

Systematics of nuclei similar to ^{67}Ge strongly suggest that the 104, 120, 122, and 243 keV gamma rays deexcite

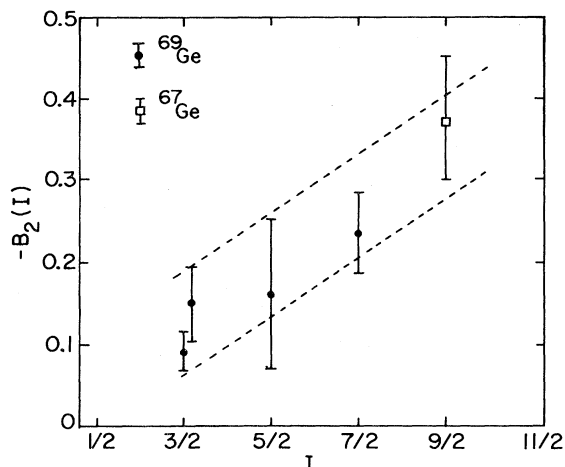


FIG. 2. The dipole orientation coefficients $B_2(I)$ measured for the $^{63,65}\text{Cu}(^6\text{Li},2n\gamma)^{67,69}\text{Ge}$ reactions, plotted versus the spin of the aligned initial state. The point at $I = \frac{9}{2}$ is for the ^{67}Ge 734-keV $L=2$ transition. The dashed lines indicate the approximate range of B_2 used to analyze the ^{67}Ge angular distributions.

$\frac{3}{2}^-$ levels, and that these transitions can only involve $\frac{1}{2}^-$, $\frac{3}{2}^-$, $\frac{5}{2}^-$, or $\frac{7}{2}^-$ states. If the spin I_1 of the initial state is $\frac{3}{2}$, then the $\lambda=4$ term in Eq. (2) is zero for any final-state spin I_2 . In this case there would ordinarily be an underdetermined problem of one measured quantity ($A_2 B_2 Q_2$) and two unknown parameters (δ and B) even if I_2 were known. It was for this reason that the B_λ were approximately measured using the analogous $^{63}\text{Cu}(^6\text{Li},2n\gamma)^{69}\text{Ge}$ distributions.

The corrected yields $Y(\theta)$ of the 232, 287, 862, and 933 keV ^{69}Ge gamma rays for each of the three angles 0° , 45° , and 90° were fit by linear least squares to

$$Y(\theta) = N [1 + \alpha_2 P_2(\cos\theta) + \alpha_4 P_4(\cos\theta)]. \quad (3)$$

The results for $B_\lambda(I_1)$ using the mixing ratios measured by Eberth *et al.*³ are plotted versus I_1 in Fig. 2. The dashed lines in Fig. 2 designate the approximate uncertainty in the B_λ 's when applied to the case of ^{67}Ge (cf. Ref. 3). (The observed spin dependence of B_2 agrees with the expectation that the highly excited states populated directly in the reaction will decay via fewer deorienting transitions to high spin states than to low spin states.)

The ^{67}Ge distributions were measured over the five angles 0° , 30° , 45° , 60° , and 90° . Figure 3 shows the total spectrum at 90° of gamma rays from the $^{63}\text{Cu} + ^6\text{Li}$ reaction—the principal reaction products in addition to ^{67}Ge are ^{67}Ga , ^{64}Zn , and ^{64}Cu . Normalized yields $Y(\theta)$ were extracted for the 104.4, 120.8, 122.7, 243.6, and 734 keV ^{67}Ge transitions.

The measured distributions of the 104, 120, 122, and 243 keV gamma rays (involving the ground state and 18.2, 122.7, and 243.6 keV levels) were tested for $L=1$ and 2 multiplicities in all possible combinations of spins $\frac{1}{2}$, $\frac{3}{2}$, $\frac{5}{2}$, and $\frac{7}{2}$, with the previously determined constraint that the 18.2-keV gamma ray is an $E2$ transition. The analysis of these distributions $Y(\theta_i)$ was done by calculating the theoretical distribution $W(\theta)$ for each possible initial and final spin, and for the corresponding minimum, middle,

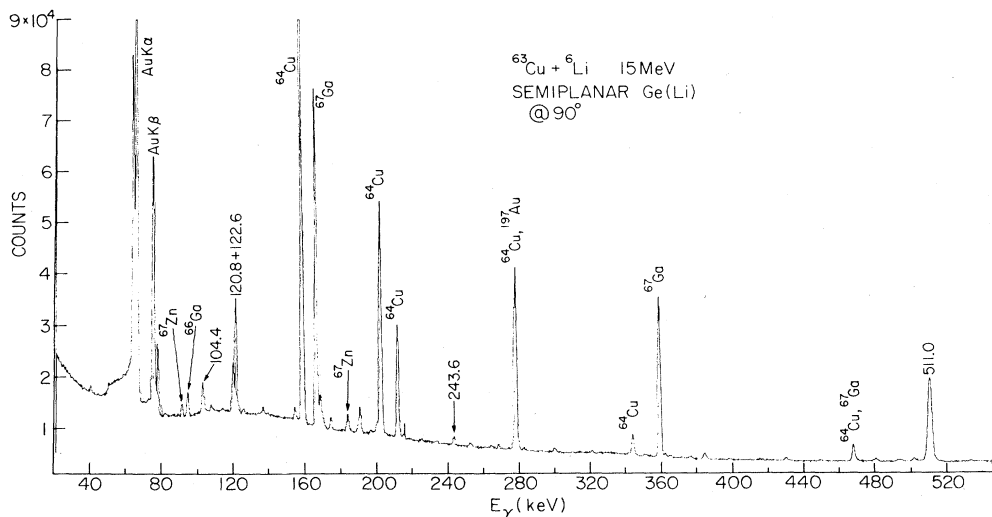


FIG. 3. The in-beam spectrum of gamma rays from the reaction $^{63}\text{Cu} + ^6\text{Li}$ observed in the semiplanar detector. The ^{67}Ge transitions are labeled by energy.

and maximum values of B_λ within the measured range, leaving δ as a free parameter. The χ^2 of each gamma-ray distribution with respect to each possible $W(\theta)$ was minimized at all values of δ in a grid $0^\circ < \tan^{-1}\delta \leq 90^\circ$ and then plotted as a function of δ . The χ^2 's are smoothly varying, quadratic functions of B_λ , and so the dependence on B_λ is well represented by the three particular values. The χ^2 plots of the $E_\gamma = 104, 120, 122,$ and 243 keV distributions for the median values of B_λ are shown in Fig. 4. A spin assignment was accepted as possible if for some δ and allowed value of B_λ the χ^2 dropped below the 0.1% confidence limit. The plots reject the possibility that the 104, 122, or 243 keV gamma rays are $\frac{5}{2} \rightarrow \frac{1}{2}$ ($L=2$) transitions.

The spins of the first four states were further con-

strained by the angular distribution of the 734-keV gamma ray, known to originate at a $\frac{9}{2}^+$ level. Al-Naser *et al.*⁵ measured its threshold to be 760 ± 11 keV, which is consistent with the threshold reported here, and establishes it as a transition to the 18.2-keV isomer. The 70 ns half-life of the $\frac{9}{2}^+$ level⁸ rules out a multipolarity $L > 3$ for the 734. The angular distribution of the 734 was tested for $L = 1, 2,$ and 3 by taking $\delta = 0$, allowing $B_2(\frac{9}{2})$ to be a free parameter, and plotting χ^2 vs B_2 for each possible multipolarity. This plot is shown in Fig. 5. The results reject $L = 1$, and clearly favor $L = 2$ over $L = 3$.

The best value for $B_2(\frac{9}{2})$ for the 752 keV state corresponds to the minimum χ^2 , and the uncertainty in B_2 is evaluated at the 31.7% confidence limit with respect to the minimum χ^2 . The 31.7% confidence limit for two pa-

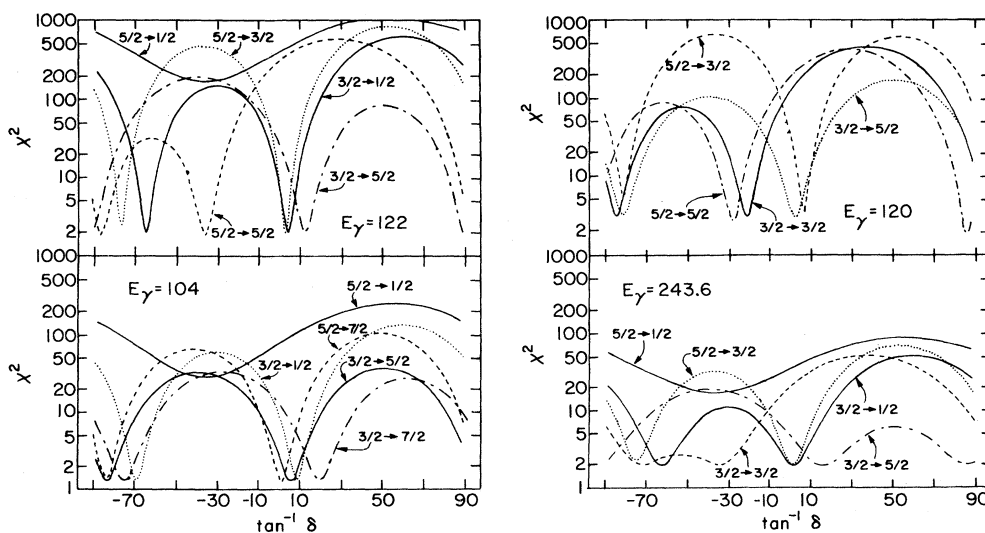


FIG. 4. The plots of χ^2 vs mixing ratio δ and spins I_1 and I_2 for the angular distributions of the 104.4, 120.8, 122.7, and 243.6 keV ^{67}Ge gamma rays. The initial and final state spin combinations which were tested are indicated on the plots. (In these plots, B_2 is the mean measured value.)

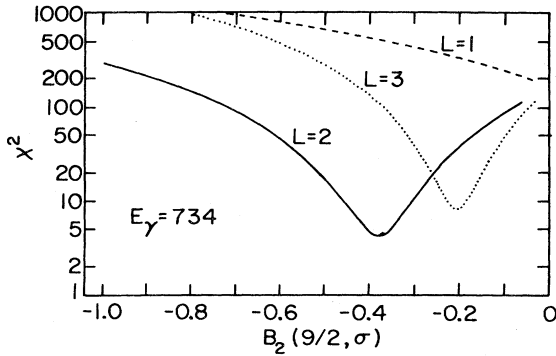


FIG. 5. The plot of χ^2 vs orientation coefficient $B_2(\frac{9}{2})$ for the angular distribution of the 734-keV ^{67}Ge gamma ray, assuming a multipolarity of $L=1, 2$, or 3 .

rameters and three degrees of freedom, in terms of the minimum χ^2 , is obtained from the F distribution according to

$$\begin{aligned}\chi_{0.317}^2 &= \chi_{\min}^2 [1 + 2/3F(0.317, 2, 3)] \\ &= 2.15\chi_{\min}^2\end{aligned}$$

(see Cline¹⁰). If the 734 keV γ ray is a pure $L=2$ transition the value

$$B_2(\frac{9}{2}) = -0.37 \pm 0.08$$

obtained in this manner agrees with the other observed orientation parameters (Fig. 2), while the value -0.20 ± 0.04 for $L=3$ is rather low. The 70 ns half-life is also consistent with an $L=2$ transition, which together with the angular distribution result provides a clear indication that the spin of the isomer is $\frac{5}{2}$. In conjunction with the other distributions, this establishes the spins of the 243.6, 122.7, 18.2, and ground states as $\frac{3}{2}^-, \frac{3}{2}^-, \frac{5}{2}^-, \frac{1}{2}^-$.

The parities of these four states can be deduced from two general observations. The first four shells accessible to the four protons and seven neutrons outside the ^{56}Ni core are (in order of increasing single-particle energy) the closely spaced $2p_{3/2}$, $1f_{5/2}$, and $2p_{1/2}$, and the more removed $1g_{9/2}$. The spin of $\frac{1}{2}$ indicates that the ground

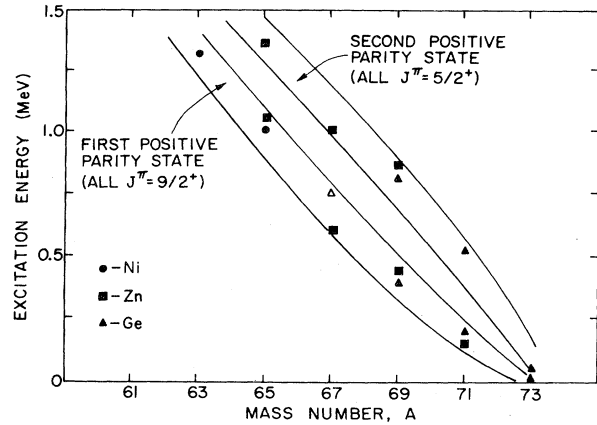


FIG. 6. The excitation energies of the first two positive-parity states of odd- A Ni, Zn, and Ge nuclei between $A=63$ and 73 .

state involves only $(\pi_{p_{3/2}})(\nu_{f_{5/2}})(\nu_{p_{1/2}})$ configurations of valence nucleons, which have negative parity. Thus the ground-state parity is negative. The $E2$ multipolarity of the 18.2-keV transition then requires negative parity for the 18.2-keV level. If the 122.7-keV level were positive parity then, regardless of the parity of the 243.6-keV level, one of the two transitions $E_\gamma=120.8$ and 243.6 keV would be $E1$ and one would be $M1$. With rare exceptions, $E1$ transitions are inhibited by factors of 10^3 – 10^7 , while $M1$ rates in this mass region are inhibited by 10^3 or less. However, the gamma-ray branching ratios for the 243.6-keV level¹ show comparable strength for the 120 and 243 keV gamma rays. Thus one of them cannot be $E1$ if the other is $M1$, and consequently the 122.7-keV level must have negative parity.

To show that the second (243.6-keV) $\frac{3}{2}$ level has negative parity, we invoke energy systematics for positive parity states in neighboring nuclei. Figure 6 shows the J^π and excitation energy of the first and second positive parity states of even- Z , odd- N nuclei from ^{63}Ni to ^{73}Ge . In all cases the first positive parity state is $\frac{9}{2}^+$ and the second is $\frac{5}{2}^+$. All of the positive parity states for the $A=67$ nuclei in Fig. 6 are far above 250 keV in a well-defined energy

TABLE III. The ^{67}Ge spins and multipole mixing ratios, from the combined results of the angular distributions and directional correlations.

E_γ	E_i	E_f	I_i	I_f	Multipolarity	δ
104.4	122.7	18.2	$\frac{3}{2}^-$	$\frac{5}{2}^-$	$M1/E2$	> 4
120.8	243.6	122.7	$\frac{3}{2}^-$	$\frac{3}{2}^-$	$M1/E2$	< -4.9
122.7	122.7	0	$\frac{3}{2}^-$	$\frac{1}{2}^-$	$M1/E2$	$0^{+0.18}_{-0.18}$ $-1.7^{+0.4}_{-0.6}$
243.6	243.6	0	$\frac{3}{2}^-$	$\frac{1}{2}^-$	$M1/E2$	$0.04^{+0.16}_{-0.16}$ $-1.7^{+0.6}_{-1.0}$
589.0	711.3	122.7	$\frac{5}{2}^-$	$\frac{3}{2}^-$	$M1/E2$	$-1.1^{+0.6}_{-2.3}$
734.0	752.2	18.2	$\frac{9}{2}^+$	$\frac{5}{2}^-$	$M2$	
897.5	1019.9	122.7	$\frac{5}{2}^-$	$\frac{3}{2}^-$	$M1/E2$	$-0.95^{+0.85}_{-2.45}$
					$E1/M2$	

trend. In addition, the ^{67}Ge $\frac{9}{2}^+$ state at 752 keV occurs at an excitation energy consistent with the first positive parity states of the other nuclei in the figure. We conclude that the 752 keV state is the first positive parity state of ^{67}Ge , and that all of the states up through 244 keV excitation are of negative parity. $\frac{1}{2}^-$, $\frac{5}{2}^-$, $\frac{3}{2}^-$, and $\frac{3}{2}^-$ are the J^π assignments which have been made in the level scheme (Fig. 1).

These spin-parity assignments confirm that the 104, 120, 122, and 243 keV gamma rays are $M1/E2$ transitions, and that the 734 keV gamma ray is an $M2$ transition. In order to extract the $E2/M1$ mixing ratios δ , $\chi^2(\delta)$ for each transition was reevaluated over the measured range of $B_2(\frac{3}{2})$. For the $\frac{3}{2}^-$ level at 243.6 keV, B_2 was taken to be -0.145 ± 0.05 (see Fig. 2). The $\frac{3}{2}^-$ level at 122.7 keV is populated 35% of the time by a 120-keV gamma ray from the 243 level. The additional deorientation which this channel might cause was accommodated by extending the lower limit for $B_2(\frac{3}{2}; 122.7 \text{ keV})$ to -0.06 . The mixing ratios δ were taken to be the values which minimize χ^2 for $B_2 = -0.14$, and the error limits were evaluated at either the 31.7% confidence limit for $B_2 = -0.14$, or at the χ^2 minima for the extreme values $B_2 \pm \sigma(B_2)$, whichever was larger. Table III summarizes

the results for the ^{67}Ge angular distributions.

D. Gamma-gamma directional correlations from an oriented source

The ^{67}Ge directional correlation measurement was by necessity made in beam rather than with a radioactive source. The alignment induced by the beam results in correlations of prompt gamma rays which are fundamentally different from gamma-gamma correlations observed with randomly oriented sources. The introduction of a preferred coordinate axis also distinguishes a variety of detector geometries, to each of which correspond a particular set of correlation equations. Complete discussions of directional correlations involving oriented sources (DCO) may be found in, e.g., Krane, Steffen, and Wheeler,¹¹ and Ferguson.¹²

The ^{67}Ge correlations were measured with both detectors in the same plane with the beam ($\phi_1 - \phi_2 = 180^\circ$). One detector was at $\theta = -90^\circ$ and the second was moved from $\theta = 0^\circ$ to 90° . For this configuration, the geometry in which $\theta_1(\gamma_1)$ is fixed at -90° and $\theta_2(\gamma_2)$ varies is designated UP1, and the geometry with variable $\theta_1(\gamma_1)$ is UP2.¹¹ The two correlation functions are

$$W_{\text{UP1}}(\theta_2) = \sum_{\substack{\lambda_1 \lambda_2 \Lambda \\ (\text{even})}} B_{\lambda_1}(I_1) A_{\Lambda}^{\lambda_2 \lambda_1}(\gamma_1) A_{\lambda_2}(\gamma_2) Q_{\Lambda}(\gamma_1) Q_{\lambda_2}(\gamma_2) \sum_{\text{even } l} g_l^{\lambda_1 \Lambda \lambda_2}(\text{UP1}) P_l(\cos \theta_2),$$

$$W_{\text{UP2}}(\theta_1) = \sum_{\substack{\lambda_1 \lambda_2 \Lambda \\ (\text{even})}} B_{\lambda_1}(I_1) A_{\Lambda}^{\lambda_2 \lambda_1}(\gamma_1) A_{\lambda_2}(\gamma_2) Q_{\Lambda}(\gamma_1) Q_{\lambda_2}(\gamma_2) \sum_{\text{even } l} g_l^{\lambda_1 \Lambda \lambda_2}(\text{UP2}) P_l(\cos \theta_1).$$

All of the geometry information is contained in the coefficients $g_l^{\lambda_1 \Lambda \lambda_2}$, which are summarized in Ref. 11.

Correlations were measured for the cascades 120-104, 120-122, 589-122, and 897-122 in ^{67}Ge , and 807-991 in ^{64}Zn . Coincidence gates were set in the spectrum of the fixed detector. The yield of the coincident gamma ray in each gate and for each angle was extracted from the gated spectrum, normalized to the integrated beam current, and corrected for geometrical anisotropy and accidental coincidences (the accidental rate was $< 8\%$ of the true coincidence rate). The resulting angular yields $Y_\gamma(\theta_i)$ were fit by least squares to the correlation functions

$$Y(\theta_i) = \alpha_0 + \alpha_2 P_2(\cos \theta_i) + \alpha_4 P_4(\cos \theta_i).$$

The fitted coefficients $\alpha_i(\gamma_k)$ and their error matrices $M = [\sigma_{\alpha_i \alpha_j}]$ were then analyzed by a graphical method¹³ to obtain the regions in the grid δ_1 vs δ_2 corresponding to the possible solutions for the mixing ratios.

To check both the experimental and analytical procedures, the cascade 807 \rightarrow 991 in ^{64}Zn was analyzed first. This is known to be a $2^+ \rightarrow 2^+ \rightarrow 0^+$ cascade, for which $\delta_2 = 0$. The current best value for δ_1 is -3.3 ± 0.7 .¹⁴ The combination of the UP1 and UP2 correlations places six constraints on four free parameters (δ_1, B, N_1, N_2), resulting in an overdetermined measurement. This measurement yielded an $E2/M1$ mixing ratio $\delta_1 = -5 \pm 1.3$ for the 807-keV gamma ray. The alignment coefficient B_2 of

the 1798-keV 2^+ level is in the range $B_2 = -0.2 \pm 0.1$ for this solution for δ_1 .

The ^{67}Ge cascades 120-104 ($\frac{3}{2}^- \rightarrow \frac{3}{2}^- \rightarrow \frac{5}{2}^-$) and 120-122 ($\frac{3}{2}^- \rightarrow \frac{3}{2}^- \rightarrow \frac{1}{2}^-$) were analyzed next to obtain new measurements of the 104, 120, and 122-keV gamma ray mixing ratios. For $I_2 = \frac{3}{2}$, the UP1 correlation has $\alpha_4 = 0$, so the UP1 yields $Y(\theta)$ were fit to straight lines versus $P_2(\cos \theta)$. The correlations were first analyzed with no constraint on B , in order to find all possible solutions for the mixing ratios. The resulting domains of admissible solutions, using $Q_1 = \delta_1^2 / (1 + \delta_1^2)$ and $Q_2 = \delta_2^2 / (1 + \delta_2^2)$ for the axes, are shown as hatched regions in Fig. 7. Also indicated in these plots are the ranges for $\delta(104)$, $\delta(120)$, and $\delta(122)$ measured in the angular distributions. $\delta_1(120)$ is the mixing ratio common to both cascades. When the correlation results are compared with those for the angular distributions, only $\delta(120) \leq -3.1$ is consistent with all of the measurements. This constrains $\delta(122)$ to near zero or negative values and $\delta(104)$ to positive values. An additional constraint was then applied to the correlations for both cascades where $\delta(120) \leq -3.1$ by (conservatively) requiring $-0.35 \leq B_2(3/2) \leq -0.05$. The domains in the plots which satisfy this additional condition are indicated by the cross-hatched regions in Fig. 7.

For all three gamma rays at least one of the two values for δ measured in the angular distributions overlaps with at least one of the solutions for the $\gamma\gamma(\theta)$ correlations. The overlapping results of the two experiments were com-

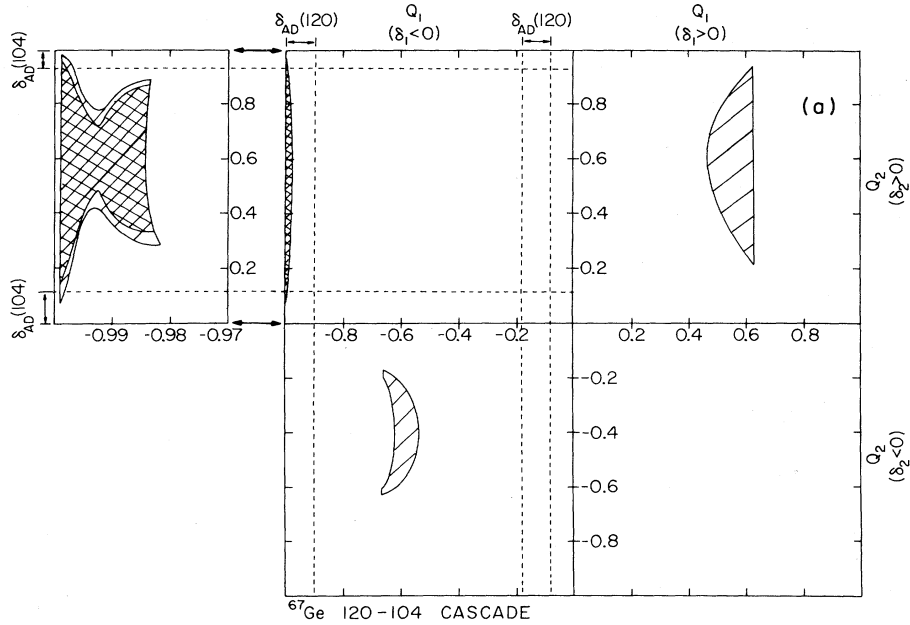


FIG. 7. The grid of solutions for (a) $Q_1(120)$ vs $Q_2(104)$, and (b) $Q_1(120)$ vs $Q_2(122)$ for the 120-104 and 120-122 ^{67}Ge cascades. The mixing ratios $\delta_{AD}(104)$, $\delta_{AD}(122)$, and $\delta_{AD}(120)$ measured in the angular distributions [converted to $Q = \delta^2(1 + \delta^2)$] are indicated on the perimeters of the graph. In the second quadrants of (a) and (b) the region $0.97 \leq Q \leq 1.0$ is enlarged for detail.

binned to obtain weighted means for the final values of the mixing ratios. The final results are summarized in Table III.

The initial state spins of the 589-122 and the 897-122 cascades (from levels at 711.3 and 1019.9 keV) were unknown. Neither of the cascades had isotropic correlations, so $I_1 = \frac{1}{2}$ was ruled out. Likewise, multipolarities $L \geq 3$ were excluded. The correlations of the two cascades were

analyzed for initial spin $I_1 = (\frac{3}{2}, \frac{5}{2}, \frac{7}{2})$; if for a particular spin I_1 no solution for (δ_1, δ_2) was found, or if the value for $\delta_2(122)$ disagreed with the previous results, then that spin was rejected. The results unambiguously determine the spins of both the 711.3 and 1019.9 keV levels to be $\frac{5}{2}$. Figure 8 shows the $\delta_1 \times \delta_2$ solutions for both cascades for $I_1 = \frac{5}{2}$ —the mixing ratio $\delta_2(122)$ is in good agreement with the earlier results.

TABLE IV. Reduced $E2$ transition rates [$B(E2)$], spectroscopic $E2$ moments (Q^S), and deformation parameters $|\beta|$ for Ni, Zn, and Ge isotopes with $32 \leq N \leq 38$.

Z	N	E^* (keV)	J^π	Q^S (fm ²)	$\frac{B(E2; i-f)}{B(E2)_{\text{Weisskopf}}}$	$ \beta $
28	32	0	0^+		14.0 ^c	0.211
28	34	0	0^+		11.6 ^c	0.193
28	36	0	0^+		11.5 ^c	0.192
28	33	0	$\frac{3}{2}^-$	+ 16.2 ^a		
28	33	67	$\frac{5}{2}^-$	- 20 ^a		
30	34	0	0^+		22.5 ^c	0.250
30	36	0	0^+		18.4 ^c	0.227
30	38	0	0^+		15.3 ^c	0.205
30	33	0	$\frac{3}{2}^-$	+ 29 ^a		> 0.143
30	33	193	$\frac{5}{2}^-$	- 12.5 ^b		> 0.068
30	35	0	$\frac{5}{2}^-$	- 2.3 ^a		0.104
30	37	0	$\frac{5}{2}^-$	+ 17 ^a		0.176
32	38	0	0^+		20.6 ^c	0.224
32	37	0	$\frac{5}{2}^-$	(\pm)2.4		

^aReference 15. ^bReference 2. ^cReference 16.

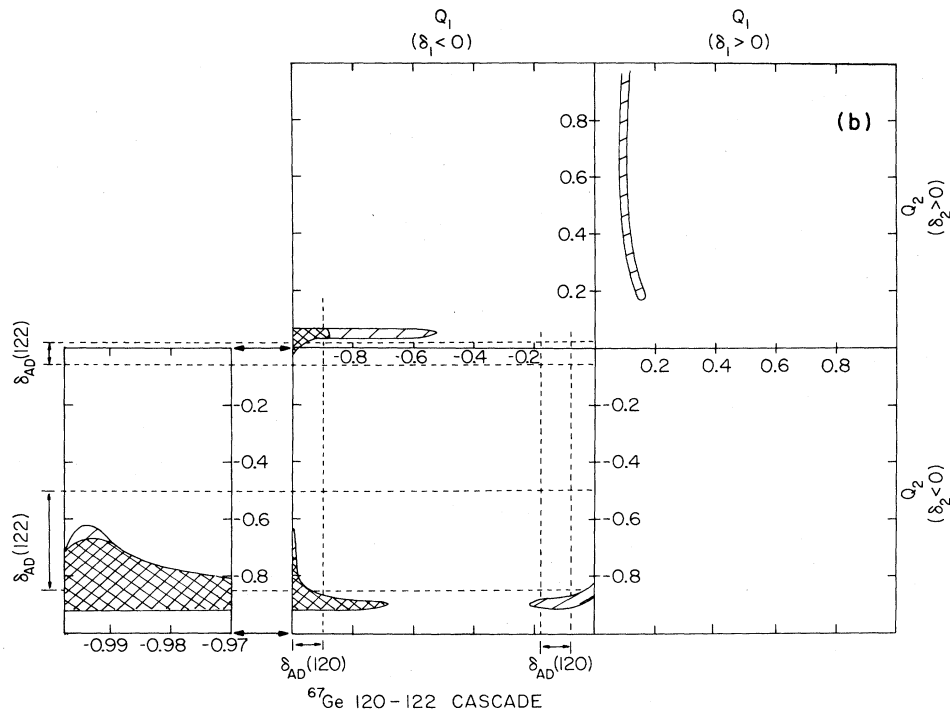


FIG. 7. (Continued.)

E. Summary of results

The experimental investigation reported here has identified 24 excited states of ^{67}Ge , and determined the spins of the ground state and levels at 18.2, 122.7, 243.6, 711.3, 752.2, and 1019.9 keV. Systematics of similar odd- A nuclei, combined with observed branching ratios for ^{67}Ge gamma rays, indicate that the first five states are negative parity. The resultant level scheme for ^{67}Ge is displayed in Fig. 1. The gamma-ray angular distribution and correlation measurements have determined the $E2/M1$ mixing ratios of six gamma rays in the level scheme; these ratios are summarized in Table III. The earlier study of low-lying levels¹ measured a lifetime of $18.50 \pm 0.3 \mu\text{s}$ and a K -shell conversion coefficient $\alpha_K = 176 \pm 29$ for the 18.2-keV $\frac{5}{2}^-$ level, thereby establishing that this level decays by an $E2$ transition.

IV. DISCUSSION

The Ge isotopes constitute a complex group of nuclei, with both the neutron and proton numbers lying between the two major shell closures at $N=28$ and 50. As a consequence, their structural and electromagnetic properties at low excitation derive from both neutron and proton shell effects, and from shape deformations connected with the departure from closed shells. These and similar nuclei in the fp shell are not as greatly deformed as, e.g., those in the actinide group, and their collective properties tend to be vibrational rather than rotational. They therefore define a transition region where neither shell nor collective effects can be expected to predominate, and where the limiting cases of the spherical single-particle shell model and

the rotational model are not valid.

In order to determine whether the low-lying excitations of ^{67}Ge and its neighbors are mainly shell excitations, or mainly collective modes, we have analyzed systematics in the structure of $^{67,69}\text{Ge}$, $^{65,67}\text{Zn}$, and $^{63,65}\text{Ni}$. In an early comparison of their low-lying level schemes a significant regularity was observed, and a systematic trend in the $B(E2)$ values for the lowest $E2$ transition was found.¹ [$B(E2)$ was reduced by a factor of ~ 10 in going from $N=35$ to 37.] It was determined in that study that the $B(E2)$ systematics were consistent with quasiparticle behavior by the valence neutrons.

As an alternative possibility, the trends could arise from changes in the shape or another collective mode of the core. The most simple collective mode for these phenomena would be a neutron coupled to an active (vibrational) and/or deformed even-even core. In order to test the $N=35$ and 37 nuclei for a particle plus core structure, we looked for correlations between the properties of the odd- A nuclei and the shapes of their $A-1$ cores. Consider the known even- A isotopes of Ni, Zn, and Ge between $N=32$ and 38. The measured $B(E2; 0^+ \rightarrow 2^+)$ (Ref. 16) values for these nuclei are summarized in Table IV, as are the deformation parameters $|\beta|$ extracted from the $B(E2)$'s. Of the corresponding odd- A isotopes, spectroscopic quadrupole moments Q^s have been measured for the ^{61}Ni , $^{63,65,67}\text{Zn}$, and ^{69}Ge ground states, and for the first excited state of ^{61}Ni . These moments are also listed in Table IV, along with a calculated² value for the $E2$ moment of ^{63}Zn 's first excited state. To obtain the deformations β of the odd- A nuclei (which are nonrotational, so that β is not directly related to Q^s), the method of Kumar¹⁷ was used to relate the intrinsic $E2$ moment Q^0 of the deformed state to the $E2$ matrix elements connecting to it; $|\beta|$ is then

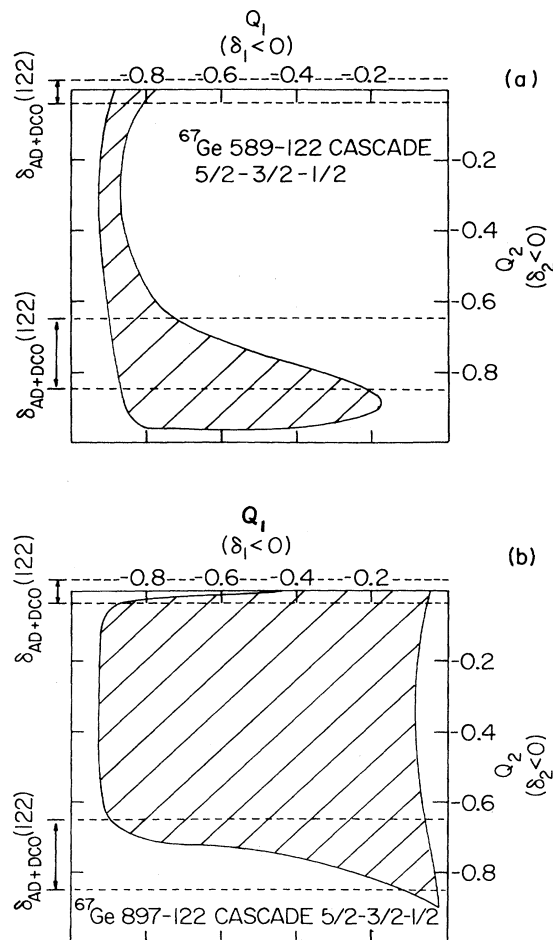


FIG. 8. The grid of solutions for (a) $Q_1(589)$ vs $Q_2(122)$ and (b) $Q_1(897)$ vs $Q_2(122)$, assuming $I_1 = \frac{5}{2}$. These are the only solutions consistent with the previously measured 122.7 γ -ray mixing ratio $\delta_{AD+DCO}(122)$.

obtained directly from Q^0 . This procedure was used to evaluate $|\beta|$ for the $^{63,65,67}\text{Zn}$ ground states and the ^{63}Zn first excited state, using for the $B(E2; i \rightarrow f)$ the measured values compiled by Van Hienen.² (There are insufficient data to determine the sign of β via Kumar's method.) These results are included in Table IV.

In Fig. 9 the $|\beta|$'s for even- A Ni and for even and odd- A Zn are plotted versus neutron number. Calculations^{2,18} of the Zn nuclei indicate that the even- A isotopes all have the same qualitative shape, so that β has the same sign for $^{64,66,68}\text{Zn}$. Thus, for the even (core) nuclei all deformations are comparable in magnitude and show the expected smooth decrease as the $N=38$ subshell closure is approached. In contrast, the deformation of the odd- A Zn ground states has a pronounced minimum at $N=35$. (The ground state spin of ^{63}Zn is $\frac{3}{2}^-$, while $^{65,67}\text{Zn}$ are $\frac{5}{2}^-$; for this reason the calculated² value for the deformation of the ^{63}Zn $\frac{5}{2}^-$ first excited state is included in the figure for completeness.) It is clear that the odd- A Zn isotope change shape in a way which is quite independent of the shapes of their $A-1$ cores. This is in contradiction to a

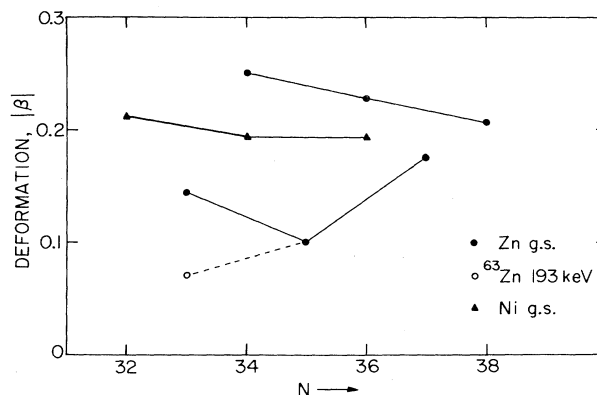


FIG. 9. The ground state deformation parameter β for $^{60,62,64}\text{Ni}$ and $^{63-68}\text{Zn}$, obtained from measured $E2$ matrix elements. Also included is β for the $\frac{5}{2}^-$ first excited state of ^{63}Zn , obtained from a shell-model calculation (Ref. 2) of the Zn isotopes.

model of the odd- A Zn nuclei as a neutron plus a vibrational or deformed core. Moreover, ^{62}Ni and ^{64}Ni possess an equal degree of deformation, while the $B(E2)$'s of the $^{63,65}\text{Ni}$ isomers differ by a factor of 10. Thus there is no obvious parallel between core shape and the $B(E2)$ trend observed for the $N=35$ and 37 isomers.

V. CONCLUSIONS

The ^{67}Ge data have established a clear similarity in the structural and electromagnetic properties of $^{63,65}\text{Ni}$, $^{65,67}\text{Zn}$, and $^{67,69}\text{Ge}$ at low excitation, which indicates that these properties derive from a common basis for all six nuclei. In consequence, a model can be accepted as valid for one of the nuclei only if it correctly describes the other five as well. As remarked earlier, these nuclei define a transitional region where shell, vibrational, and shape effects can all contribute to the overall nuclear structure. It has been shown that the $B(E2)$ systematics¹ cannot be attributed to shape transitions of an $A-1$ core. Moreover, the observed changes in shape of the odd- A Zn ground states are not correlated with similar changes in the $A-1$ cores; this rules out any type of single particle plus core structure for the $N=35$ and 37 nuclei. On the other hand, the $B(E2)$ trends are consistent with basic shell model characteristics in the $f_{5/2}$ neutron shell, as shown by the quasi-particle calculation in Ref. 1.

We conclude that the observed systematics involving the $\frac{5}{2}^-$ states are principally (neutron dominated) shell effects arising from the reconfiguration of several valence nucleons. However, the (known) deformation of these nuclei cannot be neglected in a complete model, as it is responsible for the magnitudes of the $E2$ moments and $E2/M1$ mixing ratios. (That a sufficiently large shell-model space cannot completely account for the observations is shown in the shell-model calculation of the Zn isotopes by Van Hienen *et al.*² who found it necessary to use a neutron effective charge of 2.1 to match the known quadrupole moments.) Thus a satisfactory model of nuclei in the fp shell must involve the shell effects of several valence nucleons coupled to a deformed core.

ACKNOWLEDGMENTS

The authors would like to thank Robert D. Lawson and John P. Schiffer for helpful discussions, and the staffs of the Argonne tandem accelerator and the Notre Dame Nu-

clear Structure Laboratory for their assistance in the acquisition of the data. This work was submitted in partial completion of the requirements for the Ph.D. degree at the University of Chicago. The research was supported by the U.S. Department of Energy.

*Present address: Nuclear Physics Laboratory, University of Washington, Seattle, WA 98195.

¹M. J. Murphy, C. N. Davids, E. B. Norman, and R. C. Pardo, Phys. Rev. C **17**, 1574 (1978).

²J. F. A. Van Hienen, W. Chung, and B. H. Wildenthal, Nucl. Phys. **A269**, 159 (1976).

³U. Eberth, J. Eberth, E. Eube, and V. Zobel, Z. Phys. A **273**, 411 (1975).

⁴T. Paradellis, G. J. Costa, R. Seltz, C. LeBrun, D. Ardouin, F. Guilbault, M. Vergnes, and G. Berrier, Nucl. Phys. **A330**, 216 (1979).

⁵A. M. Al-Naser, A. H. Behbehani, P. A. Butler, L. L. Green, A. N. James, C. J. Lister, P. J. Nolan, N. R. F. Rammo, J. F. Sharpey-Schafer, H. M. Sheppard, L. H. Zybert, and R. Zybert, J. Phys. G **5**, 423 (1979).

⁶W. H. Zoller, G. E. Gordon, and W. B. Walters, Nucl. Phys. **A137**, 606 (1969).

⁷V. Zobel, L. Cleemann, J. Eberth, T. Heck, and W. Neumann, Nucl. Phys. **A346**, 510 (1980).

⁸H. Bertschat, H. Haas, W. Leitz, U. Leithauser, K. Maier, H. Mahnke, E. Recknagel, W. Semmlor, R. Sielemann, B.

Spellmeyer, and T. Wickert, J. Phys. Soc. Jpn. **34**, 217 (1973).

⁹M. J. Murphy, C. N. Davids, and E. B. Norman, Phys. Rev. C **22**, 2204 (1980).

¹⁰D. Cline and P. M. S. Lesser, Nucl. Instrum. Methods **82**, 291 (1970).

¹¹K. S. Krane, R. M. Steffen, and R. M. Wheeler, Nucl. Data Tables **11**, 351 (1973).

¹²A. J. Ferguson, *Angular Correlation Methods in Gamma-ray Spectroscopy* (North-Holland, Amsterdam, 1965).

¹³M. J. Murphy, Ph.D. thesis, University of Chicago, 1980.

¹⁴D. N. Simister, G. D. Jones, A. Kogan, P. R. G. Lornie, T. P. Morrison, O. M. Mustaffa, H. G. Price, P. J. Twin, and R. Wadsworth, J. Phys. G **4**, 111 (1978).

¹⁵*Table of Isotopes*, 7th ed., edited by C. M. Lederer and V. S. Shirley (Wiley, New York, 1978), p. A42.

¹⁶P. H. Stelson, Nucl. Data **A1**, 21 (1965).

¹⁷K. Kumar, in *The Electromagnetic Interaction in Nuclear Spectroscopy*, edited by W. D. Hamilton (North-Holland, Amsterdam, 1975), p. 120.

¹⁸H. Chandra and M. L. Rustgi, Phys. Rev. C **4**, 874 (1971).